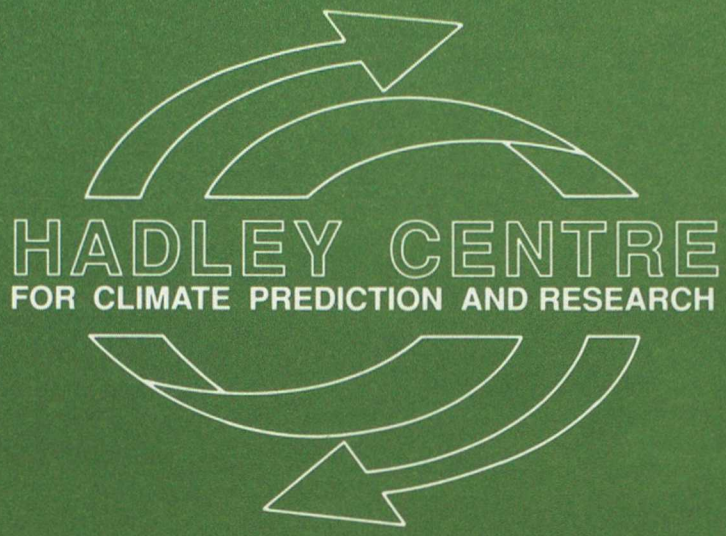

Seasonal dependence of ENSO prediction skill

by

M A Balmaseda, M K Davey and D L T Anderson

CRTN 51

September 1994

CLIMATE
RESEARCH
TECHNICAL
NOTE

Hadley Centre
Meteorological Office
London Road
Bracknell
Berkshire RG12 2SY

CLIMATE RESEARCH TECHNICAL NOTE NO. 51

SEASONAL DEPENDENCE OF ENSO PREDICTION SKILL

by

M.A. Balmaseda, M.K. Davey, D.L.T. Anderson

Hadley Centre for Climate Research and Prediction
Meteorological Office
London Road
Bracknell
Berkshire RG12 2SY
U.K.

Note: This paper has not been published. Permission to quote from it should be obtained from the Director of the Hadley Centre

Seasonal dependence of ENSO prediction skill

Magdalena A. Balmaseda *, Michael K. Davey**, David L.T. Anderson*

*: Atmospheric, Oceanic and Planetary Physics
Clarendon Laboratory, University of Oxford,
Parks Road, Oxford, OX1 3PU, England

**: Hadley Centre, Meteorological Office,
London Road, Bracknell,
Berkshire RG12 2SZ, England

Abstract

When forecasting SST in the Equatorial Pacific, most prediction schemes have a spring barrier: i.e. they have skill scores that are substantially lower when predicting northern spring and summer conditions compared to autumn and winter. We investigate this feature by examining predictions during the 1970s and the 1980s, using an ocean model of intermediate complexity coupled to a statistical atmosphere. Results show that predictions initialised during the 1970s exhibit typical prominent skill decay in spring, whereas the seasonal dependence in those predictions initialised during the 1980s is rather small. Similar changes in seasonal dependence are also found in predictions based on simple persistence of observed SST anomalies. This decadal change in the spring barrier is related to decadal variations found in the amplitude and degree of seasonal phase locking of the observed SST anomalies. Results suggest that predictive skill depends on the phase of the ENSO cycle as well as the seasonal cycle. A study of SST anomalies from 1900 to 1990 shows several changes in behaviour on a decadal scale, though the change from the 1970s to the 1980s is exceptional.

The seasonal dependence of model heat content predictions is investigated and found to be similar to that for SST, except that it shows a winter barrier rather than the spring barrier evident in SST. This difference in timing may account for the recovery in skill found in models that contain both SST and heat content information, because information is not lost from both fields simultaneously.

1. Introduction

In the last decade, considerable progress has been made in the understanding and prediction of the El Niño / Southern Oscillation (ENSO) phenomenon, which is the main climate fluctuation at interannual timescales in the tropics. The results of both numerical modelling and data analysis have shed light on the mechanisms that drive the aperiodic alternation between the cold and warm phases of ENSO (McCreary and Anderson, 1991, Neelin et al, 1994). A hierarchy of prediction schemes, ranging from pure statistical models to sophisticated coupled GCMs, has been developed: claims are made that ENSO can be successfully predicted up to one year in advance (Latif et al, 1994).

One prominent feature of the predictions of ENSO, common to most of the models, is a pronounced seasonal variation in skill. Many prediction schemes show a marked decay in skill during spring (the "spring barrier"), followed sometimes by a recovery of skill in autumn and winter. The causes and nature of the seasonal dependence still remains as an open question. Some authors (Zebiak and Cane, 1987, Battisti, 1988, Goswami and Shukla, 1991) have discussed the seasonal dependence of predictability in their models, concluding that the predictability of the system is smaller during spring because the interaction between the ocean and the atmosphere that drives interannual anomalies is weaker during this season; this explanation has been supported by results with empirical models, such as the seasonal Principal Oscillation Pattern analysis carried out by Blumenthal (1991). Webster and Yang (1992) have used observed circulation features to investigate the predictability barrier, and they suggest that interaction with the rapid spring growth of the south Asian summer monsoon may be a factor.

There is evidence (Gill and Rasmusson 1983, Kousky and Leetmaa 1989, Wang 1994) that the warm events during the 1980s are different, both in spatial distribution and timing, when compared to the canonical El Niño event described by Rasmusson and Carpenter (1982) for composites of earlier El Niño events. Motivated by these results, we try to address three main questions, by using predictive skill scores and statistical analysis of observations: (a) how does predictability differ in the '70s and the '80s?; (b) are these differences related to the interaction between the ENSO and the seasonal cycle?; (c) do these differences constitute an isolated episode or are they linked to changes occurring at interdecadal time scales?

An intermediate dynamical ocean-empirical atmosphere coupled model was used to conduct prediction experiments during the '70s and '80s, as described in section 2. Systematic differences in the prediction scores between the two decades are found (sec-

tion 3). Predictions made using simple persistence of observed sea surface temperature (SST) anomalies, described in section 4, confirm the decadal differences. Further analysis suggests that differences in ENSO during the '70s and '80s are closely related to the interaction of ENSO with the seasonal cycle. Interdecadal changes from the beginning of this century are also analysed and discussed in section 4, using observed SST.

2. Dynamical prediction experiments

Predictions were carried out using the coupled model described in Balmaseda et al. (1994), which consists of a tropical Pacific ocean model with two active layers coupled to a statistical model that relates SST anomalies and surface wind stress anomalies. (The anomalies are relative to monthly climatology.) The ocean model is first forced by observed wind stress (based on data from Florida State University (FSU), Goldenberg and O'Brien, 1981) during the period 1961-1991. The output of this simulation run is used to build the statistical atmosphere model, which assumes that the wind stress anomalies are a linear function of the first 6 Principal Components (PC) of the model SST anomalies, with seasonal variation.

The initial conditions for 92 hindcast experiments, each of 24 months duration, are taken from the simulation run at three month intervals during the period 1969-1991. Correlation skill scores r are used to evaluate the model predictions. For example, $r(SST'_{pred}, SST'_{obs})$ will denote correlation of a set of model predicted values SST'_{pred} with observed values SST'_{obs}, where $'$ denotes perturbations from monthly climatology. The observations of SST are taken from the UKMO Global Ice and Sea Surface Temperature (GISST) data set (Parker et al, 1994). The climatology is the 1951-1980 GISST average. This data set has the advantage of going back beyond the beginning of this century, which is needed for the analysis of interdecadal variability in the next section. All the analyses concerning the last two decades have also been repeated with COADS (Comprehensive Oceanic and Atmospheric Data Set, Reynolds 1988). There are no significant differences between the results obtained with the two data sets for this time period.

Correlation skill $r(SST'_{pred}, SST'_{obs})$ as a function of lead time is shown in figure 1a for the east/central equatorial region Niño3 (5°N-5°S, 150°W-90°W), where the model performance is good and comparable to other models (Latif et al. 1994). Figure 1b also shows correlations for Niño3 hindcasts, but separated according to the season at the *start* of each hindcast; clearly the predictive skill of the coupled system has a strong seasonal dependence. In agreement with other models (e.g. Zebiak & Cane 1987),

the correlation skill of the predictions decreases markedly as hindcasts pass through northern spring. Predictions initialised in spring show stable behaviour for one year, with skill declining when predicting conditions for the next spring, reaching a minimum when predicting summer. The skill of predictions starting in summer declines after 9 months, when predicting spring conditions, and so on.

Often the skill recovers after the spring decrease. This recovery of skill after the spring decay implies that whatever causes the loss of predictability at that time does not completely destroy the memory of the coupled system. The disturbance causing the drop in SST predictability might be a surface phenomenon that does not likewise influence the subsurface structure of the ocean at the same time. Thus the system could keep part of the overall structure that determines its slow evolution, and its components could recover skill, provided that the disturbance does not affect the surface and subsurface structure simultaneously. To test this hypothesis, skill has been computed for oceanic heat content (HC) anomalies, which are related to the subsurface temperature structure. The heat content here is defined as the temperature vertically integrated over the 2 active layers of the ocean model (about 275 m), scaled by mean depth to give units of temperature. Predictions ${HC'}_{pred}$ of HC anomalies are validated against values ${HC'}_{sim}$ from the model simulation forced by observed winds. This is done because we do not have reliable observations of heat content for the 23 year period considered.

Figure 2 shows correlation skills $r({SST'}_{pred}, {SST'}_{sim})$ and $r({HC'}_{pred}, {HC'}_{sim})$ for predictions of model values separated by season, using HC' in the Pacific-wide equatorial band 5°N-5°S (figure 2a), and SST' in region Niño3 (figure 2b). (Equatorial band HC' is chosen because, unlike SST' which is concentrated in the east-central Pacific, HC' variability is spread throughout the equatorial Pacific.) Like SST' in figure 1b, model HC' skill (figure 2a) has seasonal dependence, and can partially recover after a decline. The seasonal features in model SST' skill (figure 2b) are basically similar to those in figure 1b based on observations: figure 2b is included to allow closer comparison of SST' results with HC' results. (Note that correlations of model hindcasts against model simulation values are unity at zero lag.)

An important feature of figure 2 is that the decay in HC' skill happens between winter and spring, about one season before the decay in the SST' skill. For example, skill with autumn initial conditions (dashed curves in figure 2) first decreases markedly after 4 months for HC', but only after 7 months for SST'. This phase difference in the drop and recovery of predictive skill between the two variables suggests that surface and subsurface information is not lost simultaneously, as discussed above. A possible scenario is that when HC' skill declines, SST' can drive wind anomalies that force

HC' changes that allow recovery of HC' skill; and when SST' skill falls HC' can cause upwelling changes that allow recovery of SST' skill.

3. Decadal contrasts

The dynamical prediction experiments were next separated into two subsets: predictions initialized during the decade of 1970-1980, and predictions initialized during the decade 1981-1990. (It makes little difference whether the subsets are divided elsewhere in the range 1978 to 1981.) The results included in figure 1 show that there is a clear difference in the skill scores for the two decades for predictions of observed Niño3 SST', with higher scores during the '80s at lead times longer than 6 months. The seasonal dependence of the skill $r(SST'_{pred}, SST'_{obs})$ in hindcasting observed SST' differs greatly in the '70s and '80s, as shown in figure 3. For the '70s (figure 3a) there is remarkably large skill decay, starting in spring and reaching a skill minimum in summer. The skill scores always recover after the pronounced decay. The amplitude of the seasonal dependence in the skill scores is very large. By contrast, figure 3b for the '80s shows small seasonal dependence.

When skill using model simulated values is likewise calculated separately for the '70s and '80s, differences in the seasonality of the predictions between the two decades are again found, with stronger '70s seasonality for HC' and SST' compared to the '80s. Figure 4 shows the seasonal skills $r(HC'_{pred}, HC'_{sim})$ and $r(SST'_{pred}, SST'_{sim})$ for the prediction of model equatorial band HC' and Niño3 SST' for the '70s. For HC' the seasonality is particularly noticeable for lead times longer than 12 months. The phase lag between HC' and SST' skill is again evident: HC' skill starts to decay in winter and reaches a minimum in spring (figure 4a), while SST' (figure 4b) shows a skill decay in spring and a minimum during summer.

The fact that similar '70s versus '80s behaviour is found in the hindcasts of both model simulated and observed SST' indicates that the cause cannot simply be differences in SST observation between the two decades, because the model contains no observed SST anomaly information.

4. Analysis of observations

We first corroborate the results of the model predictions by using simple persistence of the observed SST anomalies to compute analogous skill scores for the same cases. Initial anomalies are held constant throughout the prediction period to obtain estimates

SST'_{per}. Correlation skills $r(SST'_{per}, SST'_{obs})$ for Niño3 SST' with initial conditions over the '70s and over the '80s are shown in figure 5: skill is clearly higher in the '80s, as was found for the dynamical model predictions (c.f. figure 1). Corresponding skill scores separated by initial season are provided in figure 6. During the '70s (figure 6a) seasonal dependence is strong, and persistence is a good predictor until spring, but in the '80s the spring decay is not as sharp and the seasonal dependence is weak. In contrast to the dynamical model results, the persistence scores do not recover after the decay.

The same calculations of the persistent behaviour of SST anomalies has been repeated for anomalies in different regions of the Pacific. Compared to Niño3, there is hardly any seasonality in the Western Pacific (Niño4), but there is stronger seasonality (and decadal differences) towards the east (regions Niño1 and 2).

There are also clear seasonal differences in variability for the '70s and '80s. Figure 7 shows time series of January, April, July and October observed Niño3 SST', together with dynamical model predictions initialized 9 months in advance. The observed SST' is particularly low in April during the '70s, and the predictions do not reproduce such a low amplitude. The standard deviation of SST anomalies organised by month-of-year is shown in figure 8 for the decades of the '70s and '80s. The '70s and '80s both have a winter maximum, but in the '70s the variability has a pronounced minimum in spring (April conditions), which is much less prominent during the '80s. (When examined separately, cold and warm anomalies show the same behaviour).

During the '70s interannual variability was strongly phase locked to the seasonal cycle, with the transition phase of ENSO (anomalies near zero) occurring in spring in region Niño3. That would explain the low spring variability of the anomalies and the spring drop in the persistence skill when passing from one phase of ENSO to the other. During the '80s, however, there seems not to be a preferred season for the transition phase, so that none of the seasons is particularly persistent (in contrast to summer in the '70s), and the variance of the anomalies does not exhibit a pronounced minimum in spring. This scenario agrees with that depicted by Wang (1994), who describes the changes in the onset of El Niño before and after the late '70s.

It seems then that there are clear differences between the interannual variability of the decades of the '70s and '80s. These differences could be related to a dramatic change in the mean state of the climate system that occurred during 1977-1978, in which large changes were noticed in the tropics and the extratropics (Trenberth, 1990, Kerr, 1992, Trenberth and Hurrel, 1994).

The question arises as to whether such decadal changes have occurred at other times. One main obstacle to answering this question is the availability of observations. The UKMO GISST dataset provides gridded values that go back beyond the beginning of this century, but the spatial coverage of actual observations has changed considerably with time. However, averaging over relatively large areas provides a method of improving the quality of the records, at the expense of a decreased spatial resolution. Figure 9 shows SST' in region Niño3 for this century, showing the main ENSO events which occurred irregularly throughout this period.

We will focus attention on three features of the interannual variability of SST that may be affected by interdecadal changes: (a) persistence of SST in the Niño3 region; (b) seasonal variations of the interannual variance; (c) eastward or westward propagation of the SST anomalies. We have defined three indices P, V and G, representative of these features. For each month-of-year m, indices $P(y_0, m)$ and $V(y_0, m)$ use information in a window centred on year y_0. ($y_0 = 1$ corresponds to 1901 etc.) The window covers 15 years ($y_0 - 7$ to $y_0 + 7$), with values in the outer 2 years at each end tapered by cosine tails. (The cosine tails simply smooth abrupt changes, and do not qualitatively affect the results.) Anomalies denoted T'' are relative to the mean within the window. The index P is the correlation of Niño3 anomalies (denoted ${T''}_3$) with values 3 months before (i.e. the correlation skill of simple persistence at a lead of 3 months). Index V is a measure of the variance within the window:

$$V(y_0, m) = \sum_{y=y_0-7}^{y_0+7} {T''}_3(12y + m)^2 W(y - y_0) \; / \; \sum_{y_0-7}^{y_0+7} W(y - y_0) \qquad (1)$$

where $W \leq 1$ is the window factor, y_0 ranges from 7 to 85, and m ranges from 1 to 12. Thus P and V contain information about seasonality: strong dependence on m indicates strong locking of interannual variability to the seasonal cycle.

The difference ${T'}_2 - {T'}_3$ is a measure of the zonal gradient of SST in the eastern Pacific, where T_2 is SST in the Niño2 region immediately west of Ecuador (0-5°S, 90°W-80°W). Suppose $r(j)$ is the correlation of ${T'}_2 - {T'}_3$ with ${T'}_3$ values j months previously, calculated using the 36 values in a 3 year window (no tapering). Index G is defined as $r(6) - r(-6)$, and provides a measure of zonal propagation ($G > 0$ for eastward, $G < 0$ for westward.) For example, during a westward propagating event a warm anomaly in Niño3 would be preceded by a positive zonal gradient in the east Pacific ($r(6) > 0$) and followed by a negative gradient ($r(-6) < 0$). Note that G would be positive for warm or cold westward moving anomalies.

Figure 10 shows the values of P, V and G since the beginning of this century. In the '70s and '80s, P and V demonstrate the features discussed above. In the '70s P has large seasonality with a prominent spring barrier: an autumn/winter maximum is followed by a sharp decline to a minimum when predicting spring conditions. When '80s information dominates the window there is a switch to low seasonality, with P larger on average than in the '70s. In the '80s P has a winter maximum and autumn minimum, but is irregular through the rest of the year. In the '70s V has large seasonality, with a sharp decrease from winter to spring followed by gradual recovery, giving a sawtooth profile. By contrast, in the '80s V seasonality is lower and there are both spring and autumn minima. The index G shows westward movement in the '70s, with a switch to eastward with the onset of the major 82/83 event.

Generally, P and V have winter maxima, with a rapid decline in V going into spring. Several changes in P and V behaviour in this century are also apparent in figure 10, with relatively abrupt (i.e. in 2 or 3 years) shifts followed by stable behavior for about 10 years. Early this century V and P have moderate seasonal range, with summer minima. Around 1916 there is a shift to exceptionally low V, and irregular P seasonality with a strong semiannual component. (This new behaviour is not due to the absence of interannual variability, but rather is due to lack of seasonal phase locking. In Fig. 9 it can be seen that several cold events occur in 1915-25, but each extremum occurs in a different season.)

Around 1926 there is shift back to a regime like the early 1900s. Then around 1936 P decreases and is very irregular for a couple of years: in figure 9 it can be seen that this is a period of low interannual variability. During the '40s P has larger seasonal range, with a near-zero minimum that varies between autumn and spring. Then in the late '40s there is a shift to irregular P with low seasonality, as found in the '20s (and '80s). In the late '50s there is a return to large P seasonality that lasts through the '60s and '70s. In terms of the seasonal range of V and P, the largest values this century occur in the '70s.

The zonal direction index G is mostly negative (indicating westward propagation), often is below -0.5, and is sometimes below -1 (e.g. 1924/25, and 1965/66). There are occasional brief positive episodes (e.g. around 1910, 1928, 1936, 1949), with the only strong sustained eastward event ($G > 1$) being in 1982/83. There is no obvious connection between direction and the seasonal phase-locking of interannual variability measured by V and P.

5. Summary and discussion

Predictions of SST anomalies in region Niño3 from a coupled model with a dynamical ocean component, were analysed. The correlation skill shows a pronounced drop during spring conditions, often followed by a recovery. The recovery suggests that the coupled system keeps part of its memory despite the spring loss of SST skill. This idea is supported by results from predictions of the oceanic heat content HC: correlation skill for HC tends to decay in winter and then partially recover, so HC and SST information is not lost simultaneously. For example, interannual SST anomaly information can drive winds that help HC to recover; and HC evolution can alter SST via upwelling changes that lead to recovery of SST skill.

Dynamical predictions were made for the '70s and '80s. (Reliable wind data needed for predictions for earlier decades was not available). To investigate possible long-term changes in predictability, these predictions were separated into two subsets, initialized during the '70s and '80s respectively, with each subset containing at least two warm ENSO events. Large differences in the seasonality of the predictions between the two decades are found; the spring SST skill decay is large and coherent in the '70s, but small and not so coherent for predictions initialized during the '80s. The same results are obtained for predictions made using simple persistence of observed SST anomalies.

Analysis of the observations indicates that the pronounced spring barrier in the '70s is accompanied by a marked minimum in the spring variance; during the '80s, when the predictive skill shows weak seasonality, the seasonality of the variance is also weak. The coherent relationship between the seasonality in predictions and variance suggests that they are connected by the degree of phase locking of ENSO to the seasonal cycle: when seasonal phase locking is strong (e.g. if the transition phase consistently occurs in a particular season, so that there is a minimum in variance associated with that season) then predictions also show a strong seasonal barrier (i.e. a sharp decline in skill when forecasting conditions for that season). A possible consequence of this relation is that prediction schemes that overemphasise seasonal phase locking will also exaggerate the seasonal prediction barrier, thus limiting their predictive skill. The changes in behaviour from the '70s to the '80s also suggest that ENSO predictive skill may depend as much on the phase of ENSO as on the background seasonal cycle (c.f. the idealised model by Davey et al. 1993).

Motivated by the variations found in the skill of ENSO predictions during the '70s and '80s, the seasonality and predictability of interannual SST anomalies in the tropical Pacific were investigated using SST data from 1900 to 1990. SST anomalies for

standard equatorial regions were used to define indices of interdecadal variability. Index P measures persistence correlation skill within a decadal window, retaining seasonal variations; index V similarly measures variance within the same window. Index G is used to detect changes in the zonal propagation of the anomalies. Indices P and V reveal interdecadal variability in both predivtive skill and in seasonal phase locking of the ENSO cycle. In most of this century there is moderate to strong locking of interannual variability to the seasonal cycle, with winter maxima in V and P followed by rapid declines. This type of behaviour was most pronounced in the '70s. Seasonality is relatively weak and irregular in the late '10s and early '20s, in the '50s, and in the '80s. Most of the record shows westward propagation (i.e. anomalies moving westward from the South American coast), with the only major eastward signal being in the early '80s.

Such results should be treated with caution, as data coverage through this century is variable. The indices do suggest, however, that ENSO characteristics such as seasonal phase locking do vary on a decadal timescale, and that there may consequently be decadal fluctuations in predictability. The causes of such changes require further investigation.

Acknowledgement:

Thanks are due to Mike Jackson and the Climate Data group at the Hadley Centre for creating and supplying the GISST dataset.

Balmaseda, M.A., Anderson, D.L.T., and Davey M.K., 1994: ENSO prediction using a dynamical ocean model coupled to statistical atmospheres. *Tellus*, to appear

Battisti, D.S., 1988: Dynamics and thermodynamics of a warming event in a coupled tropical atmosphere-ocean model. *J. Atmos. Sci.* **45** 2889-2919.

Blumenthal, M.B., 1991: Predictability of a coupled ocean-atmosphere model. *J. Climate* **4** 766-784.

Davey, M.K., Anderson, D.L.T., and Lawrence, S.P., 1993: A simulation of seasonality in ENSO forecast skill. UKMO ClimRes. Tech. Note No. 38.

Gill, A.E. and Rasmusson, E.M., 1983: The 1982-83 climate anomaly in the equatorial Pacific. *Nature* **306** 229-234.

Goldenberg, and O'Brien, 1981: Time and space variability of tropical Pacific wind stress. *Mon. Wea. Rev.* **109** 1190-1207.

Goswami, B.N. and Shukla, J., 1991: Predictability of a coupled ocean-atmosphere model. *J. Climate* **4** 3-22.

Kerr, R.A., 1992: Unmasking a shifty climate system *Science.* **225** 1508-1510.

Kousky, V.E. and Leetmaa, A., 1989: The 1986-87 Pacific warm episode: evolution of oceanic and atmospheric anomaly fields. *J. Climate* **2** 254-267.

Latif, M., Barnett, T.P., Cane, M.A., Flügel, M., Graham, N.E., von Storch, H., Xu, J.-S., and Zebiak, S.E., 1994: A review of ENSO prediction studies. *Climate Dynamics.* **9** 167-179.

McCreary, J.P. and Anderson, D.L.T., 1991: An overview of coupled ocean-atmosphere models of El Niño and the Southern Oscillation. *J. Geophys. Res.* **96** 3125-3150.

Neelin, J.D., Latif, M., and Jin, F.-F., 1994: Dynamics of a coupled ocean-atmosphere models: The tropical problem. *Annu. Rev. Fluid Mech.* **26** 617.

Parker, D.E., Folland, C.K., Bevan, A., Ward, M.N., Jackson, M. and Maskell, K., 1994: Marine surface data for analysis of climatic fluctuations on interannual to century timescales. In: Natural Climate Variability on Decade to Century Time Scales Eds D.G. Martinson, K. Bryan, M. Ghil, M.M. Hall, T.R. Karl, E.S. Sarachik, S. Soroostian and L.F. Talley. National Academy Press, Washington.

Rasmusson, E.M. and Carpenter, T.H., 1982: Variations in tropical sea surface temperature and surface wind fields associated with the Southern Oscillation / El Niño. *Mon. Wea. Rev.* **110** 354-384.

Reynolds, R.W., 1988: A real-time global sea surface temperature analysis. *J. Climate* **1** 75-86.

Trenberth, K.E., 1990: Recent observed interdecadal climate changes in the Northern hemisphere. *Bull. Am. Met. Soc.* **71** 988.

Trenberth, K.E., and Hurrel, J.W., 1994: Decadal atmosphere-ocean variations in the Pacific. *Climate Dynamics* **9** 303-319.

Wang, B., 1994: Interdecadal Changes in El Niño onset in the last four decades. *J.Climate*, submitted

Webster, P.J., and Yang, S., 1992: Monsoon and ENSO: selectively interactive systems. *Quart. J. Roy. Met. Soc.* **118** 877-926.

Zebiak, S.E. and Cane, M.A., 1987: A model El Niño - Southern Oscillation. *Mon. Wea. Rev.* **115** 2262-2278.

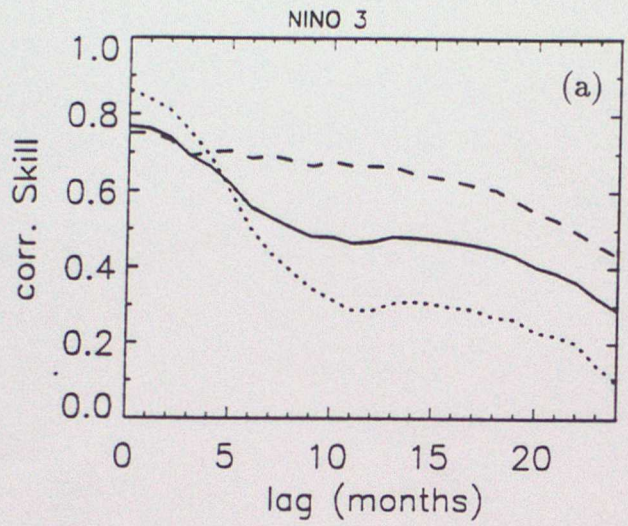

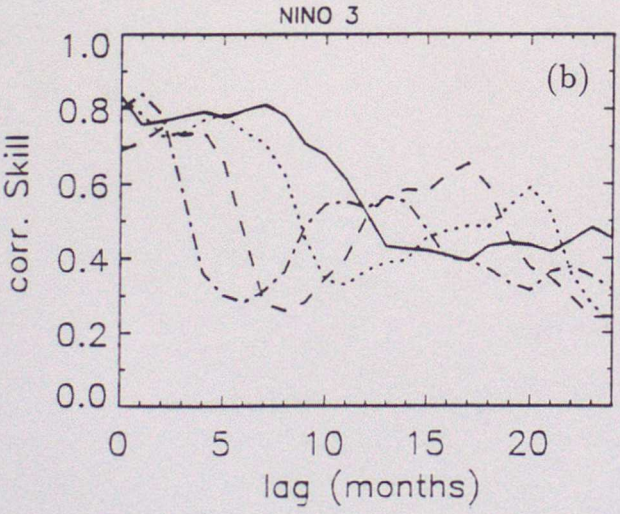

Fig. 1: Correlation skill: correlation of observed and predicted (dynamical model) SST anomalies in region Niño3, as a function of lead time. Predictions are made at 3 month intervals.

(a) using all data from the periods 1970-1990 (solid), 1970-1980 (dotted) and 1980-1990 (dashed). Conditions during the '80s are predicted better.

(b) data from 1970-1990, separated according to the season when the model prediction was initialised and started: in northern spring (solid), summer (dotted), autumn (dashed) and winter (dot-dashed). There is a clear decrease in skill when predicting spring and summer conditions.

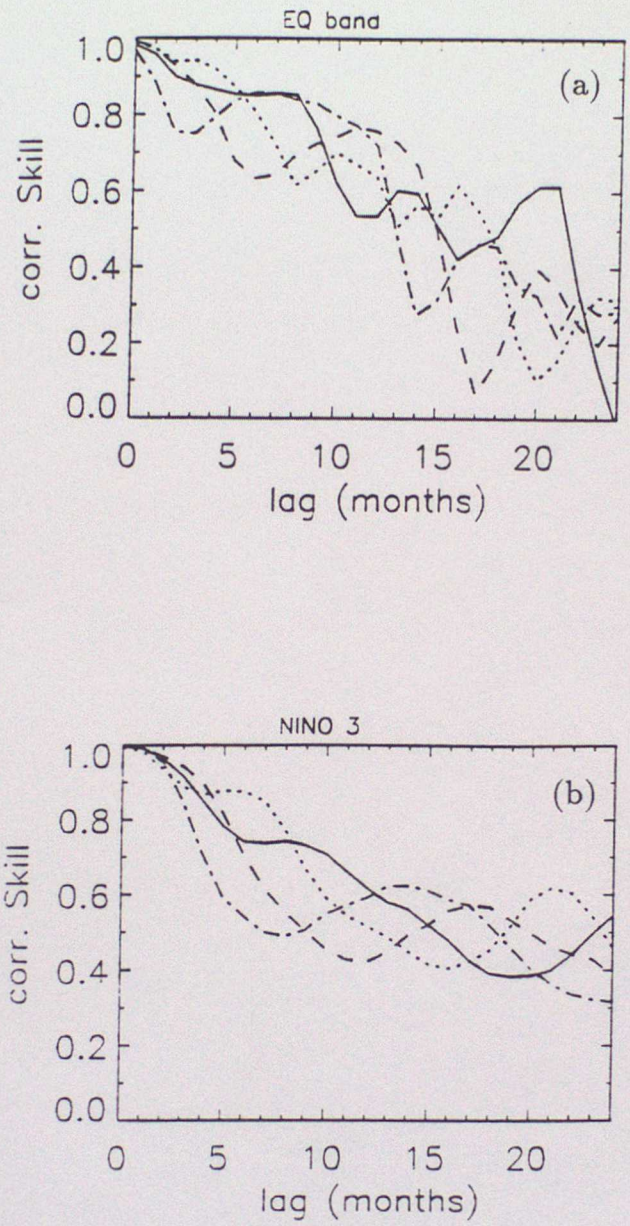

Fig. 2: Correlation skill: correlation of ocean values simulated (forced using observed winds) and predicted by the dynamical model. Data from 1970-1990, separated according to the season when the model prediction was initialised and started: in northern spring (solid), summer (dotted), autumn (dashed) and winter (dot-dashed).

(a) model heat content HC anomalies averaged along the equatorial band 5N-5S 130E-70W

(b) model SST in region Niño3.

Note that the decay of HC skill occurs one season before the decay of SST skill: there is a winter HC barrier and a spring SST barrier.

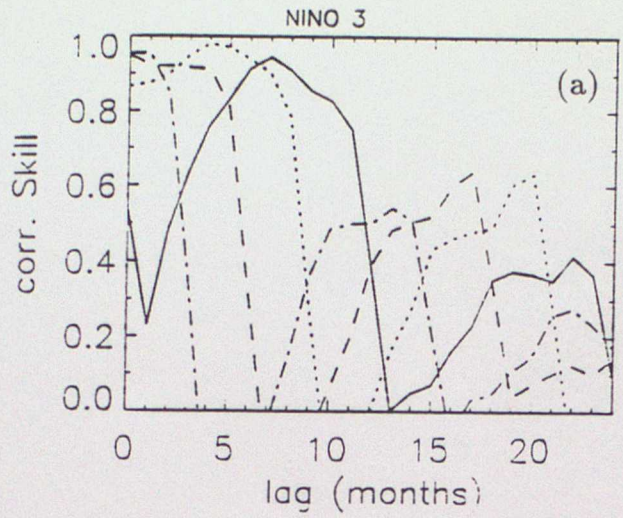

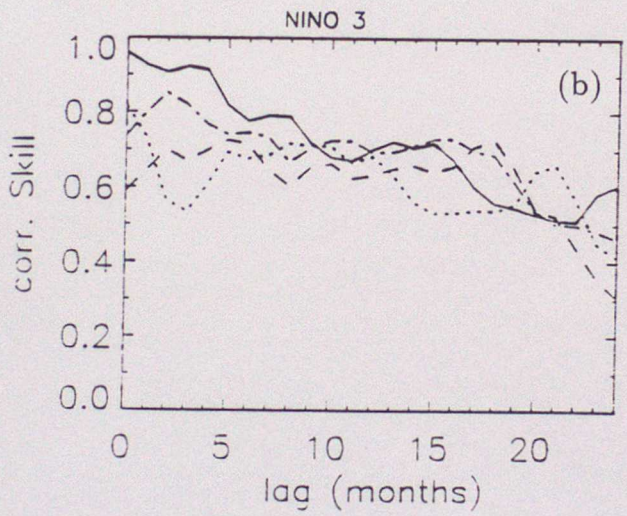

Fig. 3: Correlation skill: correlation of observed and predicted (dynamical model) SST anomalies in region Niño3, as a function of lead time. Predictions are made at 3 month intervals. Data separated according to the season when the model prediction was initialised and started: in northern spring (solid), summer (dotted), autumn (dashed) and winter (dot-dashed).

(a) data from the 1970s, (b) data from the 1980s

During the '70s there is strong seasonality, with minimum skill when predicting spring and summer conditions. The seasonality of the predictions during the '80s is much weaker.

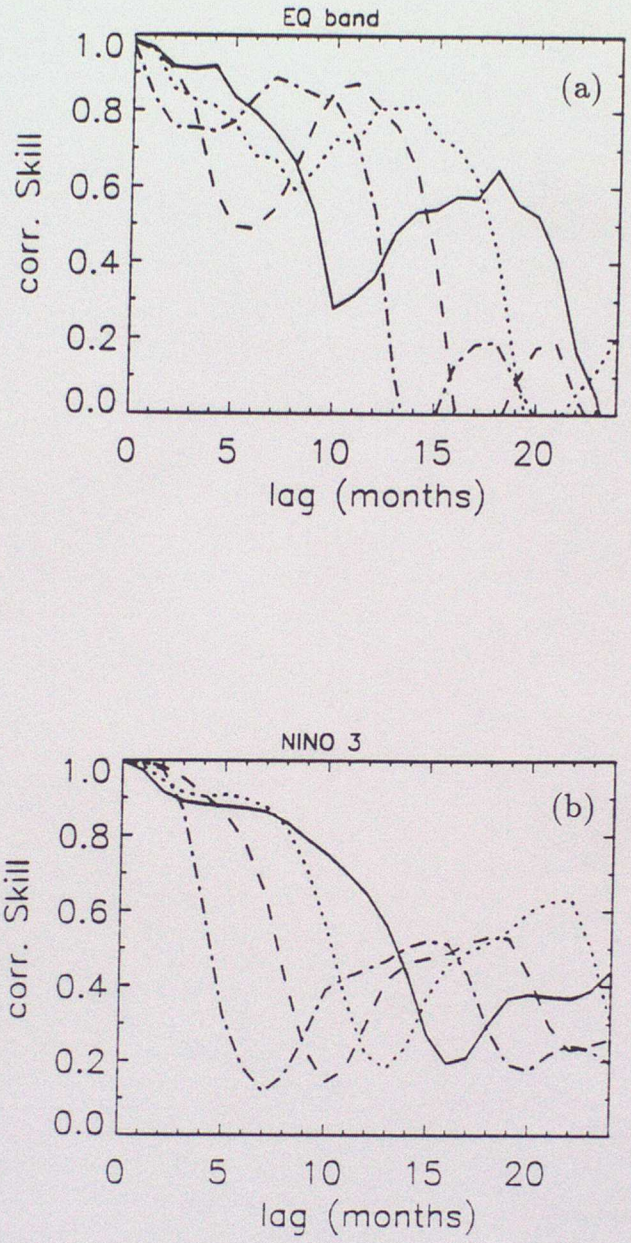

Fig. 4: Correlation skill: correlation of ocean values simulated (forced using observed winds) and predicted by the dynamical model. Data from 1970-1980, separated according to the season when the model prediction was initialised and started: in northern spring (solid), summer (dotted), autumn (dashed) and winter (dot-dashed).

(a) model heat content HC anomalies averaged along the equatorial band 5N-5S 130E-70W.

(b) model SST in region Niño3.

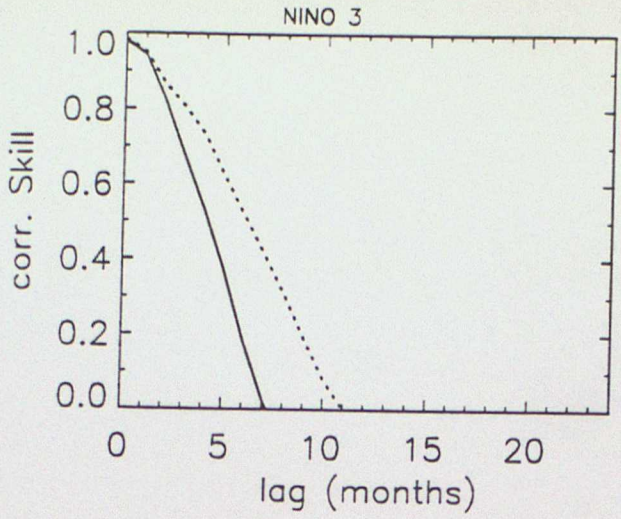

Fig. 5: Correlation skill: correlation of observed and predicted (simple persistence) SST anomalies in region Niño3, as a function of lead time. Predictions are made at 3 month intervals, using all data from the periods 1970-1980 (solid) and 1980-1990 (dotted).

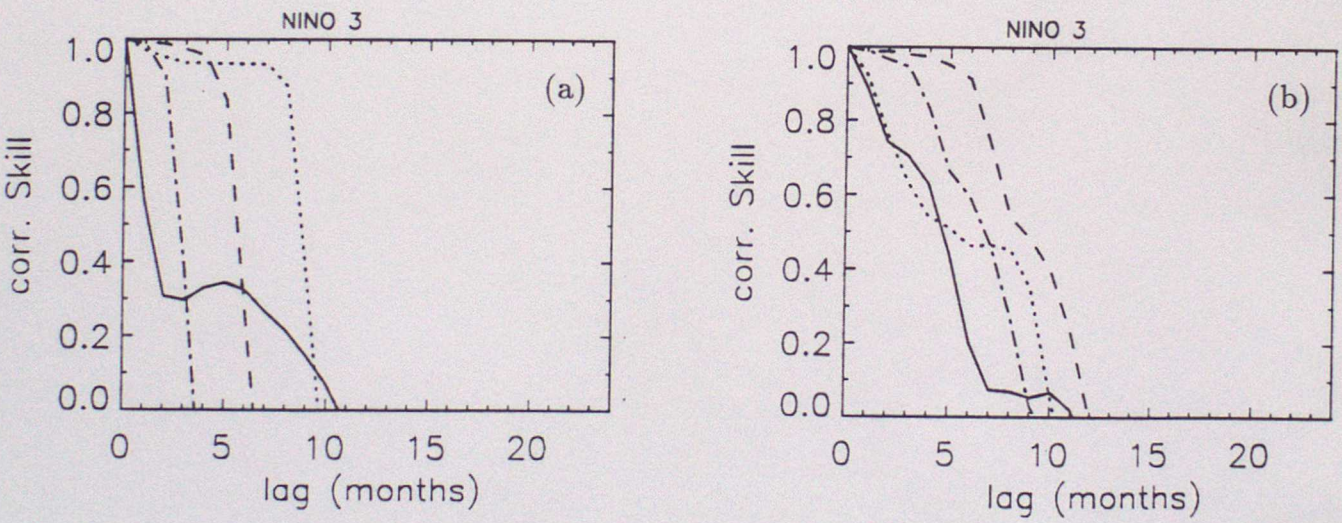

Fig. 6: Correlation skill: correlation of observed and predicted (simple persistence) SST anomalies in region Niño3, as a function of lead time. Predictions are made at 3 month intervals. Data separated according to the season when the prediction was started: in northern spring (solid), summer (dotted), autumn (dashed) and winter (dot-dashed).

(a) data from the 1970s.

(b) data from the 1980s.

In the '70s skill decays abruptly when predicting spring and summer conditions, and does not recover. Initial summer conditions persist for several months. There is much less seasonal contrast in the '80s.

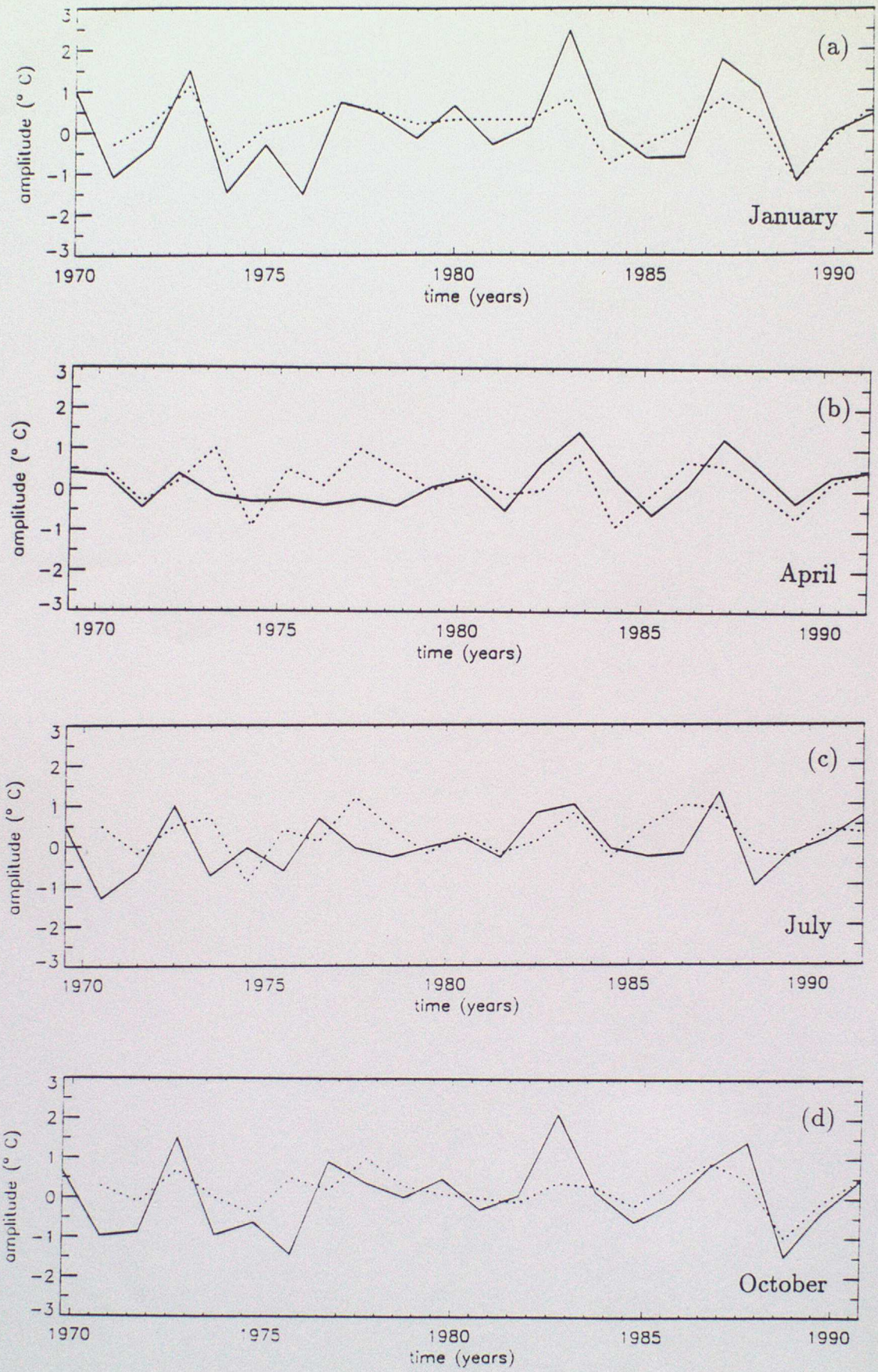

Fig. 7: Observed (solid line) and predicted (dynamical model initialised 9 months before, dotted line) SST anomalies in region Niño3 during different seasons: (a) January; (b) April; (c) July and (d) October. Note the low amplitude of the observed April anomalies during the '70s.

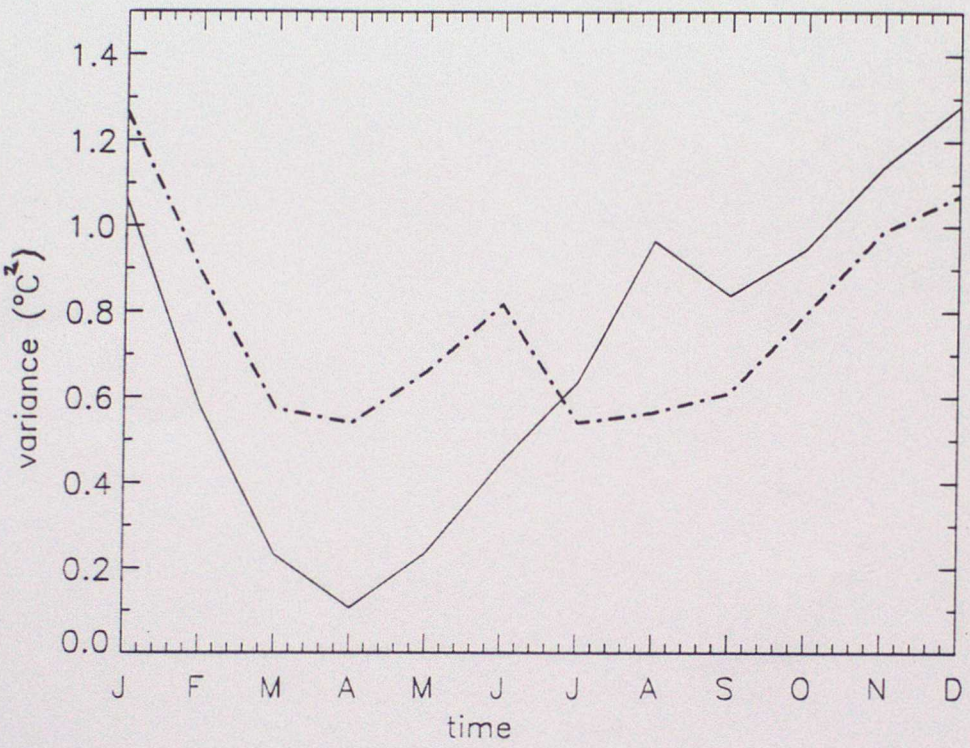

Fig. 8: Variance of observed SST anomalies in region Niño3, versus month-of-year, calculated for the '70s (solid line) and the '80s (dash-dot).

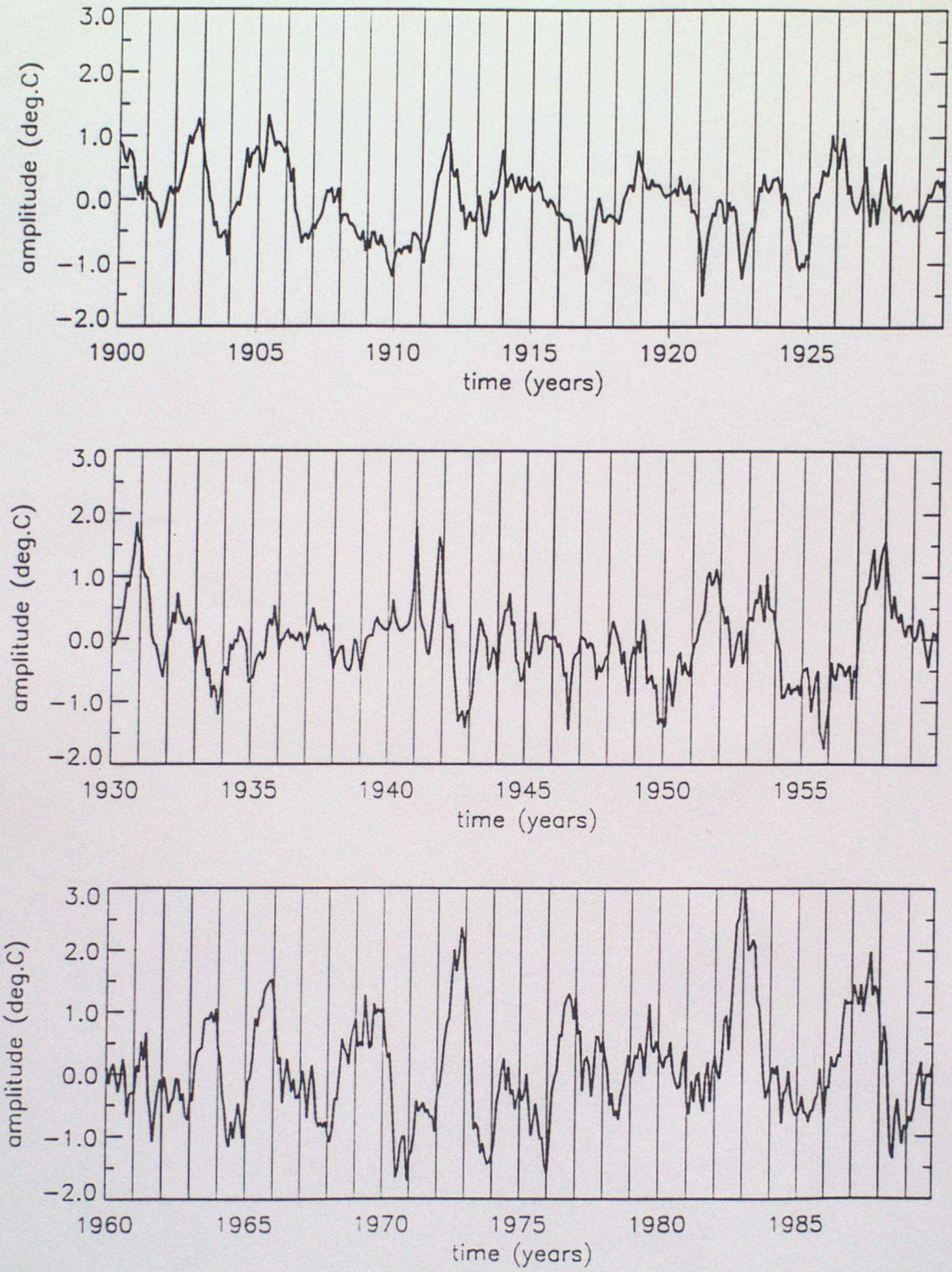

Fig. 9: Observed SST anomalies in region Niño3 for 1900 to 1990. Vertical lines correspond to the start of each year.

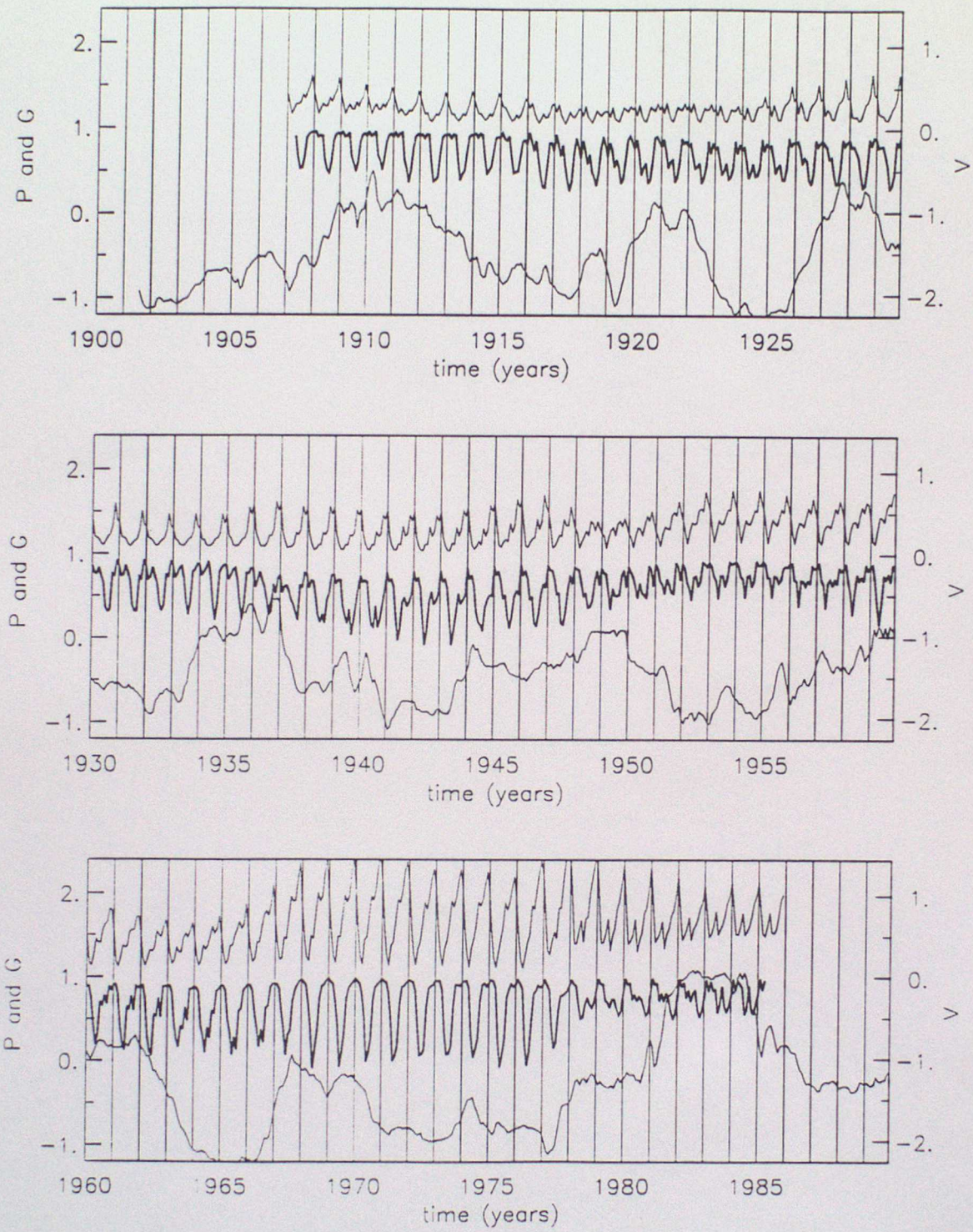

Fig. 10: Time evolution of persistence skill index P (thick curve), variance index V (upper thin curve) and zonal propagation index G (lower thin curve) during this century (see text for definitions). Vertical lines correspond to the start of each year. The scale for P and G is on the left, and on the right for V.

CLIMATE RESEARCH TECHNICAL NOTES

CRTN 1	Oct 1990	Estimates of the sensitivity of climate to vegetation changes using the Penman-Monteith equation. P R Rowntree
CRTN 2	Oct 1990	An ocean general circulation model of the Indian Ocean for hindcasting studies. D J Carrington
CRTN 3	Oct 1990	Simulation of the tropical diurnal cycle in a climate model. D P Rowell
CRTN 4	Oct 1990	Low frequency variability of the oceans. C K Folland, A Colman, D E Parker and A Bevan
CRTN 5	Dec 1990	A comparison of 11-level General Circulation Model Simulations with observations in the East Sahel. K Maskell
CRTN 6	Dec 1990	Climate Change Prediction. J F B Mitchell and Qing-cun Zeng
CRTN 7	Jan 1991	Deforestation of Amazonia - modelling the effects of albedo change. M F Mylne and P R Rowntree
CRTN 8	Jan 1991	The role of observations in climate prediction and research. D J Carson
CRTN 9	Mar 1991	The greenhouse effect and its likely consequences for climate change. D J Carson
CRTN 10	Apr 1991	Use of wind stresses from operational N.W.P. models to force an O.G.C.M. of the Indian Ocean. D J Carrington
CRTN 11	Jun 1991	A new daily Central England Temperature series, 1772-1991. D E Parker, T P Legg and C K Folland
CRTN 12	Jul 1991	Causes and predictability of Sahel rainfall variability. D P Rowell, C K Folland, K Maskell, J A Owen, M N Ward

CLIMATE RESEARCH TECHNICAL NOTES

CRTN 13	Jul 1991	Modelling changes in climate due to enhanced CO2, the role of atmospheric dynamics, cloud and moisture. C A Senior, J F B Mitchell, H Le Treut and Z-X Li
CRTN 14	Sep 1991	Sea temperature bucket models used to correct historical SST data in the Meteorological Office. C K Folland
CRTN 15	Aug 1991	Modelling climate change, and some potential effects on agriculture in the U.K. P R Rowntree, B A Callander and J Cochrane
CRTN 16	Aug 1991	The Boreal Forests and Climate G Thomas and P R Rowntree
CRTN 17	Aug 1991	Development of a Stratosphere-Troposphere Data Assimilation System. R Swinbank.
CRTN 18	Sep 1991	A study of asynchronous coupling using a simple climate model. M K Davey.
CRTN 19	Sep 1991	The Oceanic Carbon Cycle. N K Taylor
CRTN 20	Nov 1991	Worldwide ocean-atmosphere surface fields in Sahel wet and dry years using provisionally corrected surface wind data. M N Ward
CRTN 21	Dec 1991	Coupled tropical ocean global atmosphere models at the UKMO. M K Davey, C Gordon, S Ineson and S Lawrence
CRTN 22	Dec 1991	Empirical parameterisation of tropical ocean-atmosphere coupling. M Allen, M K Davey, D L T Anderson and P D Killworth
CRTN 23	Feb 1992	The temporal evolution of Equatorial Currents in the Indian Ocean D L T Anderson, D J Carrington, R A Corry and C Gordon
CRTN 24	Feb 1992	Stratospheric analyses provided by the U.K. Meteorological Office M J Bailey, A O'Neill and V D Pope

CLIMATE RESEARCH TECHNICAL NOTES

CRTN 25	Feb 1992	Modelling interannual variability in the Indian Ocean using momentum fluxes from the UKMO and ECMWF operational weather analyses. D L T Anderson and D J Carrington
CRTN 26	Mar 1992	A GCM simulation of the impact of Amazonian deforestation on climate using an improved canopy representation J Lean and P R Rowntree
CRTN 27	Mar 1992	The parameterization of rainfall interception in GCMs A J Dolman and D Gregory
CRTN 28	Jun 1992	Development of worldwide marine data eigenvectors since 1985 A W Colman
CRTN 29	Jun 1992	A tropical ocean model with reduced physics M K Davey
CRTN 30	Jun 1992	International Temperature Workshop, Boulder, Colorado, USA, 16 January 1992 Edited by D E Parker
CRTN 31	Jul 1992	Simulation of clear-sky outgoing longwave radiation over the oceans using operational analyses A Slingo and M J Webb
CRTN 32	Sep 1992	A prediction of the transient response of climate J M Murphy
CRTN 33	Nov 1992	LEPS scores for assessing climate model simulations and long-range forecasts. C K Folland
CRTN 34	Jan 1993	Stratospheric Data Assimilation System Guide Editer: R Swinbank
CRTN 35	Mar 1993	A Stratosphere-Troposphere Data Assimilation System R Swinbank and A O'Neill
CRTN 36	Mar 1993	Validation of hydrological schemes for climate models against catchment data. P R Rowntree and J Lean

CLIMATE RESEARCH TECHNICAL NOTES

CRTN 37	Apr 1993	Modelling of palaeoclimates: Examples from the recent past J F B Mitchell
CRTN 38	May 1993	A simulation of seasonality in ENSO forecast skill M K Davey, D L T Anderson and S Lawrence
CRTN 39	Jul 1993	ENSO Prediction experiments using a simple ocean-atmosphere model D-H Wu, D L T Anderson and M K Davey
CRTN 40	Sep 1993	Diagnosis of dynamic sea-surface and sea-level changes from the Cox ocean model J M Gregory
CRTN 41	Sep 1993	Seasonal variations of the clear-sky greenhouse effect: the role of changes in atmospheric temperatures and humidities M J Webb, A Slingo and G L Stephens
CRTN 42	Nov 1993	Sea-level changes under increasing atmospheric CO_2 in a transient coupled ocean-atmosphere GCM experiment. J M Gregory
CRTN 43	Dec 1993	Global and regional patterns of climate change: recent predictions for the Arctic P R Rowntree
CRTN 44	Feb 1994	The effect of changing horizontal diffusion in the atmospheric version of the unified climate model C D Hall and R A Stratton
CRTN 45	Mar 1994	Simulation of El-Niño/Southern Oscillation like variability in a global AOGCM and its response to CO_2 increase. S F B Tett
CRTN 46	Apr 1994	Global data required for monitoring climate change. D E Parker and C K Folland
CRTN 47	May 1994	Seasonal uptake of anthropogenic CO_2 in an ocean general circulation model. N K Taylor

CLIMATE RESEARCH TECHNICAL NOTES

CRTN 48	Jun 1994	A tropic-wide oscillation of boreal summer rainfall and patterns of sea-surface temperature. M N Ward, K Maskell, C K Folland, D P Rowell and R Washington
CRTN 49	Jun 1994	Simulation of the tropical Pacific using a simplified ocean model M A Balmaseda, D L T Anderson and M K Davey
CRTN 50	Sep 1994	Simulation of global mean temperature using a box-diffusion climate model P R Rowntree
CRTN 51	Sep 1994	Seasonal dependence of ENSO prediction skill M A Balmaseda, M K Davey and D L T Anderson